

Inscription of Polymer Optical Fiber Bragg Grating at 962 nm and Its Potential in Strain Sensing

Zhi Feng Zhang, Chi Zhang, Xiao Ming Tao, *Member, IEEE*, Guang Feng Wang, and Gang Ding Peng

Abstract—Fiber Bragg grating (FBG) with a 962-nm Bragg wavelength was fabricated in trans-4-stilbenemethanol doped poly(methyl methacrylate) polymer optical fibers (POFs) using a phase mask with 17% zeroth-order diffraction for the inscription wavelength of 325 nm. The effect of zeroth-order diffraction of the phase masks on FGB in POF was first examined by observing micrographs of the gratings. A linear relationship between the fiber axial strain and shift of the FBG was observed up to 6.5% tensile strain with a strain sensitivity of 0.916 pm/ $\mu\epsilon$. However, this shift was notably affected by the time-dependent stress relaxation in the fiber, especially when the FBG was subject to a relatively higher strain $>2\%$.

Index Terms—Fiber Bragg grating (FBG), fiber grating fabrication, measurement of strain, polymer optical fiber (POF).

I. INTRODUCTION

FIBER Bragg gratings (FBGs) in silica-based optical fibers have been widely studied and applied in optical devices like fiber filters, switches and lasers, measurement of stress and strain, health-monitoring of composites and infrastructures, etc. [1], [2]. However, silica-based optical fibers are limited by low ductility. The low ductility hinders their applications for measuring large deformations, while high modulus leads to relatively low sensitivities in strain for sensing applications. FBGs in polymer-based optical fibers offer a potential solution because optical polymer like poly(methyl methacrylate) (PMMA) has a larger measurable strain range [3], [4].

The first FBG in polymer optical fiber (POF) was inscribed in PMMA fibers with a PMMA copolymer core by the modified phase mask technique to suppress the zeroth-order diffraction of phase mask [5]. In order to enhance the photosensitivity and reduce ultraviolet (UV) degradation, trans-4-stilbenemethanol (trans-SBM) was used as an active dopant in PMMA optical fibers and the photosensitivity of such fibers was systematically investigated. FBGs were written at 1550 nm from these

Manuscript received July 08, 2010; revised July 29, 2010; accepted August 15, 2010. Date of publication August 26, 2010; date of current version October 06, 2010. This work was supported in part by the Hong Kong Research Institute of Textiles, Apparel Ltd. (Grant RD/GH/PR/002/07 and Grant GHP/043/07TP) and in part by The Hong Kong Polytechnic University (Grant BB6P). The work of Z. F. Zhang was supported by a postgraduate scholarship received from The Hong Kong Polytechnic University.

Z. F. Zhang, C. Zhang, X. M. Tao, and G. F. Wang are with the Institute of Textiles and Clothing, The Hong Kong Polytechnic University, Hong Kong, China (e-mail: tctaoxm@polyu.edu.hk).

G. D. Peng is with the School of Electrical Engineering and Telecommunications, University of New South Wales, Sydney 2052, Australia.

Color versions of one or more of the figures in this letter are available online at <http://ieeexplore.ieee.org>.

Digital Object Identifier 10.1109/LPT.2010.2069090

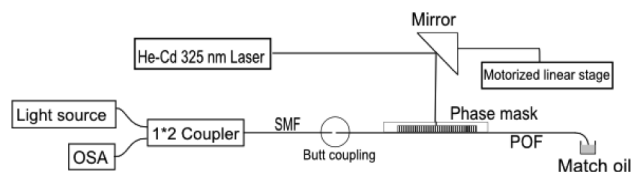


Fig. 1. Schematic diagram of grating inscription system.

fibers by the phase mask technique [6], [7]. Since then FBGs in micro-structured POFs doped with trans-SBM were reported [8]. In the previous studies, the central Bragg wavelength of the FBGs was all around 1550 nm, while at this wavelength, doped PMMA or the PMMA copolymers have larger attenuation than at lower wavelengths [9]. This is disadvantageous as only a few centimeters of POF can be used in measurements. For most practical applications, a longer length of POF is more desirable. Hence, a polymer FBG at shorter Bragg wavelength with lower material attenuation is preferred.

II. GRATING FABRICATION

The trans-SBM-doped photosensitive POFs for grating inscription were fabricated by a two-step process or pre-form drawing technique as previously reported [10]. The core/cladding diameter ratio of the fiber is 8/130, which is close to 8/125 of a single-mode silica optical fiber (SMF) to guarantee good coupling between SMF and POF.

Polymer FBGs were fabricated by the phase mask technique using a 325-nm He–Cd laser (Kimmon IK3802R-G). The total laser output is 90 mW. The experiment setup is shown in Fig. 1. The laser beam was focused, reflected, and irradiated onto the side of the fiber through a phase mask, which is placed parallel to the fiber without a gap between them. The mirror was fixed on a motorized linear stage so that the laser beam could be scanned along the length of the POF to obtain longer FBGs than the beam width (1.48 mm). The reflection spectrum of FBG was monitored during the inscription process by using a broadband light source, optical spectrum analyzer [(OSA) Ando AQ6315A] and a 1 × 2 3-dB coupler. The light was coupled into the POF from a single-mode silica optical fiber by the butt coupling with assistance of acrylic matching liquid ($n = 1.4917$).

A 10-mm-long FBG was written with phase mask (Bragg Photonics, pitch = 647 nm) in a POF with a diameter of 180 μm . The laser beam scanning speed was set to be 4 $\mu\text{m/s}$; hence, the Bragg grating took about 15 min of scanning to achieve its saturation. Reflection and transmission spectra were captured by an OSA with 0.05-nm resolution. Typical spectra of an FBG are shown in Fig. 2. Some side peaks appear at shorter wavelengths, which may be caused by the multimode nature of

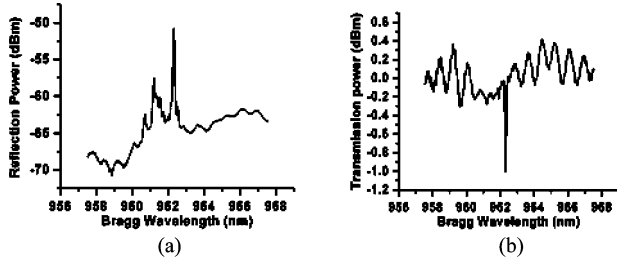


Fig. 2. (a) Reflection spectrum of POF Bragg grating at 962 nm; (b) Transmission spectrum of POF Bragg grating at 962 nm.

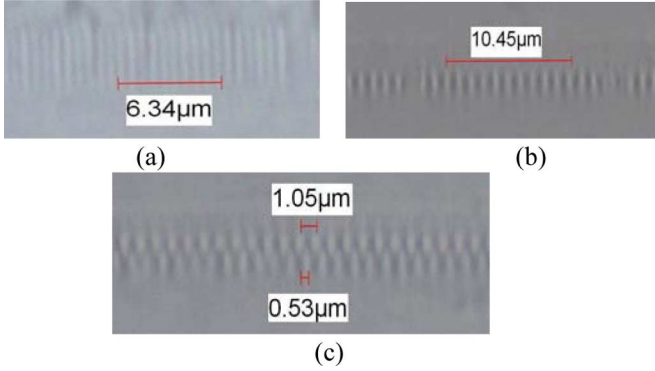


Fig. 3. (a) Microscope picture of the 962-nm polymer FBG. (b) The initial uniform grating structure of 1551-nm polymer FBG. (c) The nonuniform grating structure of the 1551-nm polymer FBG.

the fiber working at 962 nm, because the fiber was designed and fabricated as single mode at 1550 nm by optimizing the refractive index difference between the core and cladding. The current maximum reflectivity of POF grating achieved is 60% at a Bragg wavelength of 1551 nm. The reflectivity of the grating at 962 nm is approximately 20%. Further investigation is under way for improvement. Moreover, the refractive index modulation amplitude of the grating region can be estimated to be 1.5×10^{-5} by the following equations:

$$R = \tanh^2(\Omega L)$$

$$\Omega = \frac{\pi \cdot \Delta n \cdot \eta(V)}{\lambda}$$

where R is the reflectivity of the grating, L is the length of the grating, Ω is the coupling coefficient, σ is the coupling coefficient, Δn is the index modulation, and $\eta(V)$ represents the fraction of the integrated fundamental-mode intensity contained in the core.

In addition, the internal structure of the grating was observed by using an optical microscope with 100X objective oil lens, as shown in Fig. 3(a). The measured grating period was 634 nm, which was approximately equal to the phase mask pitch, not half of it as initially expected. This can be explained from the effects of the zeroth-order diffraction of the phase mask on polymer Bragg gratings. The operating wavelength of the phase mask used to inscribe 962-nm Bragg gratings was 248 nm, and its zeroth-order diffraction for 325 nm was measured to be as high as 17%, with 26% -1 st order and 25% $+1$ st order diffraction. In silica optical fibers, the FBG's period is normally expected

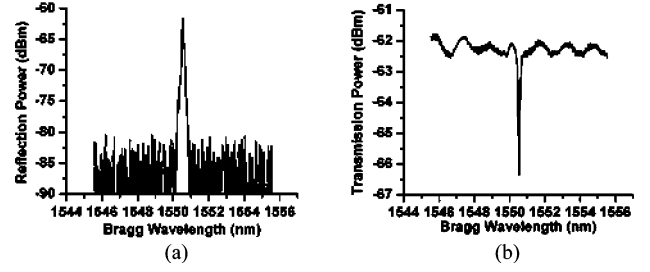


Fig. 4. (a) Reflection spectrum of POF Bragg grating at 1551 nm. (b) Transmission spectrum of POF Bragg grating at 1551 nm.

to be half of the pitch of the phase mask, when the zeroth-order diffraction of the phase mask is lower than 5% [11], [12]. The structure of polymer bulk material at micro- or nano-scales differs greatly from the silica because the nature of polymer chain entanglement. Based on computational analysis of near field interference pattern and experimental studies of surface relief grating fabricated by phase mask technology, Xiong *et al.*, [13] claimed that at the condition of considering first-order diffraction only, even a low zeroth-order diffraction (0.1%) makes the grating interference fringe pattern become a nonuniform periodic structure. The stronger the zeroth-order diffraction, the lower visibility of the grating fringe at the half of the phase mask period would be. Upon this theorem, in our POF, the possible explanation of the abnormal period of 962-nm grating fringe can be given; thus, because the 17% zeroth-order diffraction was high, it made the visibility of fringes at half period too low to be observed from the microscope.

To validate our hypothesis, a second FBG with the central wavelength at 1551 nm, shown in Fig. 4, was fabricated by using a phase mask (Ibsen Photonics) of 1045.6-nm period, which is designed for 325-nm laser.

The measured zeroth-order diffraction of this phase mask was only 1% with 26% -1 st order and 25% $+1$ st order. This grating was observed under an optic microscope. At the beginning, one uniform grating pattern appeared, with a period of 1.045 μm which is the same as the phase mask period. When the microscope focused deeper into the fiber, the other grating pattern with the same period clearly came out [see Fig. 3(b), (c)]. The second grating has a shift approximately half of the period of the first one, which means the first and second grating can just form a single nonuniform grating. This observation in POF made a good agreement with the AFM results of the grating on the surface of bulk PMMA material reported by Xiong *et al.*, so we can confirm the zeroth-order diffraction effect of the phase mask exists in polymer FBGs and this effect is the principal causation of the abnormal grating period we observed in 962-nm polymer FBGs.

III. STRAIN MEASUREMENT

After the grating inscription, the strain responses of the polymer FBGs were studied. The POF with Bragg grating was glued to a silica optical fiber to form a device by using UV-curable optical glue (Norland 76). The device was then fastened on a motorized linear stage rig for strain test (as shown in Fig. 5). Upon the test results, although Bragg wavelength shift is quasi-linearly related to strain when the fiber stretched (Fig. 6),

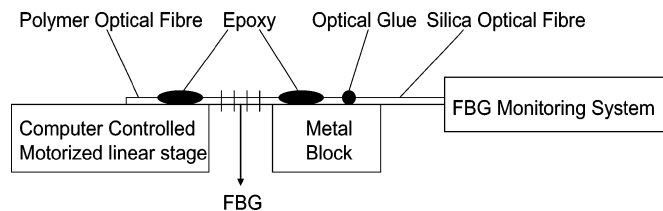


Fig. 5. Strain testing rig for POB Bragg grating.

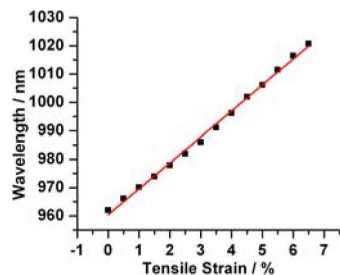


Fig. 6. Bragg wavelength shift of a polymer FBG versus fiber strain.

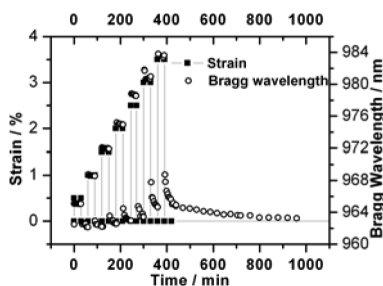


Fig. 7. Time-dependent Bragg wavelength shift of polymer FBG.

it is also dependent on the strain history of the fiber (Fig. 7). The sensitivity of the grating is $0.916 \text{ pm}/\mu\epsilon$ at 962 nm , which is comparable to $1.15 \text{ pm}/\mu\epsilon$ at 1550 nm for silica FBGs. The linear relationship extends to strain of 6.5% . To the author's knowledge, this strain range is the largest among the entire POF-based Bragg grating devices and silica optical fiber-based counterparts. This indicates that the 962-nm POF Bragg grating device may be applied potentially as large strain sensors.

When the strain is larger than 2% , the viscoelasticity of the polymer fiber becomes noticeable, and the Bragg wavelength shift is obviously time-dependent. The shift did not reverse immediately after the fiber was released from loading. For example, it took several hours for the Bragg wavelength to shift back after the fiber was stretched to 3.5% and released. A possible solution to this problem is to embed the FBG region into an elastic material with a lower viscosity to form a device. For practical applications, the device is normally mounted or embedded properly into a structure, no matter if it is rigid or soft. When a large strain is applied to the structure, the elongation of the polymer fiber in the device should be limited to its elastic

region by the virtual of structural design. A good example is a knitted fabric where the fiber strain is less than 0.5% while the fabric is uni-directionally stretched over 50% [14]. The fiber grating should follow the recovery of the elastic structure. This will be further investigated in a separate paper.

A POF Bragg grating with 962-nm reflection wavelength was fabricated using a 647-nm phase mask with 17% zeroth-order diffraction for 325-nm laser. The effect of the zeroth-order diffraction of the phase mask on polymer FBG was examined by observing and analyzing the micrographs of the grating. The strain responses of the polymer FBGs were investigated by stretching the POF up to 6.5% and a maximum 60-nm Bragg wavelength shift was observed. Viscoelasticity became noticeable when the applied strain was larger than 2% .

REFERENCES

- [1] A. Inoue, M. Shigehara, M. Ito, M. Inai, Y. Hattori, and T. Mizunami, "Fabrication and application of Fiber Bragg grating—A review," *Optoelectron. Devices Technol.*, vol. 10, pp. 119–130, 1995.
- [2] K. O. Hill and G. Meltz, "Fiber Bragg grating technology fundamentals and overview," *J. Lightw. Technol.*, vol. 15, no. 8, pp. 1263–1276, Aug. 1997.
- [3] S. Kiesel, K. Peters, T. Hassan, and M. Kowalsky, "Large deformation in-fiber polymer optical fiber sensor," *IEEE Photon. Technol. Lett.*, vol. 20, no. 6, pp. 416–418, Mar. 15, 2008.
- [4] C. C. Ye, J. M. Dulieu-Barton, D. J. Webb, C. Zhang, G. D. Peng, A. R. Chambers, F. J. Lennard, and D. D. Eastop, "Applications of polymer optical fiber grating sensors to condition monitoring of textiles," *Proc. SPIE*, vol. 7503, pp. 75030M–75030M, 2009.
- [5] G. D. Peng and P. L. Chu, "Polymer optical fiber photosensitivities and highly tunable fiber gratings," *Fiber Integrated Opt.*, vol. 19, pp. 277–293, 2000.
- [6] J. M. Yu, X. M. Tao, and H. Y. Tam, "Trans-4-stilbenemethanol-doped photosensitive polymer fibers and gratings," *Opt. Lett.*, vol. 29, pp. 156–158, Jan. 2004.
- [7] X. M. Tao, J. M. Yu, and H. Y. Tam, "Photosensitive polymer optical fibers and gratings," *Trans. Inst. Measurement Control*, vol. 29, pp. 255–270, 2007.
- [8] D. J. Webb, K. Kalli, K. Carroll, C. Zhang, M. Komodromos, A. Argyros, M. Large, G. Emilianov, O. Bang, and E. Kjaer, "Recent developments of Bragg gratings in PMMA and TOPAS polymer optical fibers—art. no. 683002," in *Proc. Advanced Sensor Systems and Applications III*, Beijing, China, 2008, p. 83002.
- [9] J. L. Manfred, "Plastic optical fibers: Properties and practical applications," *Proc. SPIE*, vol. 5596, p. 299 C308, 2004.
- [10] J. M. Yu, X. M. Tao, and H. Y. Tam, "Fabrication of UV sensitive single-mode polymeric optical fiber," *Opt. Mater.*, vol. 28, pp. 181–188, 2006.
- [11] D. Z. Anderson, V. Mizrahi, T. Erdogan, and A. E. White, "Production of in-fiber gratings using a diffractive optical element," *Electron. Lett.*, vol. 29, pp. 566–568, 1993.
- [12] K. O. Hill, B. Malo, F. Bilodeau, D. C. Johnson, and J. Albert, "Bragg gratings fabricated in monomode photosensitive optical fiber by UV exposure through a phase mask," *Appl. Phys. Lett.*, vol. 62, pp. 1035–1037, 1993.
- [13] Z. Xiong, G. D. Peng, B. Wu, and P. L. Chu, "Effects of the zeroth-order diffraction of a phase mask on Bragg gratings," *J. Lightw. Technol.*, vol. 17, no. 11, pp. 2361–2365, Nov. 1999.
- [14] S. W. Lam, P. Xue, X. M. Tao, and T. X. Yu, "Multi-scale study of tensile properties and large deformation mechanisms of polyethylene terephthalate fibre/polypropylene matrix knitted composites," *Comp. Sci. Tech.*, vol. 63, no. 10, pp. 1337–1348, 2003.